Auger, resonant, and plasmon-assisted charge-transfer processes in atom-surface collisions

M. A. Vicente Alvarez and V. H. Ponce
Comisión Nacional de Energía Atómica, Centro Atómico Bariloche and Instituto Balseiro, 8400-Bariloche, Argentina

E. C. Goldberg
INTEC, Universidad Nacional del Litoral, Guemes 3450, 3000-Santa Fe, Argentina
(Received 17 October 1997; revised manuscript received 28 January 1998)

The Keldysh Green's-function formalism is used to evaluate the atomic occupation number of a projectile colliding with a metal surface. This formalism has an advantage that allows us to handle simultaneously Auger, resonant, and plasmon-assisted exchange processes along with the interference between them. A time-dependent Hamiltonian containing Auger-like and resonantlike terms, and the electron-electron Coulomb potential in the solid, is proposed. The atomic self-energies are calculated up to a second order in the interaction potential. An effective resonant amplitude is defined, and Auger self-energies are presented where the plasmon-assisted processes are included through a surface response function. Finally, some numerical results for a proton colliding with an Al surface by using a simplified description of the solid response function are presented, where an analysis in terms of the incidence angle and the energy level is shown. [S0163-1829(98)05820-2]

I. INTRODUCTION

The scattering of ions and atoms by solid surfaces is a collisional process where many-body interactions together with complex dynamical aspects of the collision are involved. Existing experimental data over many different projectile-target combinations[1–4] reveal the importance of the study of ion-surface collisions to determine the structure of both projectile and target. The resonant and the Auger neutralization mechanisms have been currently assumed as the available ones. In the first case, a high-lying level of the ion at the valence-band energies is neutralized by one surface electron. Thus a one-electron description is adequate because the solid relaxation effects are small. For low-lying levels there are no single-electron transfers that can preserve the energy of the system. In this case an electron of the surface makes the transition to the low-lying level of the incoming ion, and the potential energy is transferred to a second electron of the surface, which is ejected. This two-electron process is the Auger neutralization channel. But there is experimental evidence of other multielectron channels, in which an electron is captured by the ion, and the energy released in the process is absorbed by some surface collective excitation.[5] It is observed that, for low-energy He^+ and Ne^+ projectiles scattered from Al and Mg surfaces, the plasmon-assisted neutralization is more important than the Auger neutralization mechanism. Furthermore, the remarkable excitation of bulk plasmons cannot be ascribed to the projectile penetrating the solid, since bulk plasmon structures are dominant even at collision energies as low as 30 eV.

During the last years great progress in the theoretical treatment of the electron exchange problem for ions moving in free-electron-like solids has been achieved. The linear response approximation (LRA) Ref. 6 and the density-functional approach are commonly used to describe ions interacting with a solid.[7] In an ion-surface collision, the sudden turn on and off of the electron exchange interaction rends difficult the use of such formalisms, and a time-dependent approach becomes indispensable. First, rate-equations models were used to calculate the atomic charge fractions with different levels of sophistication.[8] In these models the rate coefficients are calculated assuming an instantaneous interaction between the atom and the solid, therefore, the dynamical effects of the exchange process are disregarded.

The pioneering paper of Keldysh,[9] in which an analogy to the usual Feynman technique is developed for calculating Green's functions for time-dependent Hamiltonians, serves as the starting point for the treatment of nonequilibrium problems. In 1976, Blandin, Nourtier, and Hone applied this formalism to the calculation of the atomic population for a time-dependent resonant exchange process.[10] Since then, a growing number of papers was devoted to the study of one-electron transfer within the Keldysh formalism. Resonant and quasiresonant channels were considered to simulate experimental results in slow ion-surface collisions.[11–13] For projectiles that have a chance of being negatively charged during the collision, the intra-atomic interaction has been also treated by using the Keldysh formalism.[14]

On the other side, the Auger and plasmon-assisted channels have been studied in the past years within a rate-equation framework. Snowdon *et al.* calculated total rates for both resonant tunneling and Auger transfer for a static H^+ ion near a jellium surface.[15] Almulhem and Girardeau proposed the surface-plasmon-assisted exchange process, and calculations of the matrix elements for this process have been performed within a fixed-ion approximation.[16] Zimmy *et al.* analyzed the interplay of resonant and Auger processes in proton neutralization for grazing incidence. Both channels were considered on an equal footing within the rate-equation approach.[17] Recent works show that a correct description of the solid response function that includes the collective and electron-hole pair excitations leads to a good agreement with the experimental results.[18]

As far as we know, the only attempt to apply the Keldysh

formalism approach to the treatment of the Auger exchange channel was done by Makoshi and Kaji in 1991.[19] In this paper they calculated the second-order self-energy for a Hamiltonian with a time-dependent Auger-like potential. They focused on the slow ion collision case, and used the wide-band approximation to justify the use of the rate-equation approach when the band is wide enough compared to the energy scale of the particle motion.

In this paper we present an *ab initio* approach based on the Keldysh Green's-function formalism that unifies the resonant tunneling with the Auger and plasmon-assisted electron exchange mechanisms. A time-dependent Hamiltonian with surface symmetry is proposed, and the Keldysh Green's function for the atomic state is calculated through its Dyson equation. The self-energy is obtained by using the Feynman diagrammatic technique up to a second order in the interaction potential. The plasmon-assisted processes appear when the Auger lines in the diagrammatic expansion are screened by the Coulomb potential as in the *GW* approximation.[20] This yields a surface susceptibility function that simulates the response of the surface as in the LRA, by using Auger and plasmon-assisted processes as nonseparable excitations of the surface.[21] The great advantage of this approach is that it allows one to improve in a systematic way the calculation of the atomic population by including more terms in the series expansion of the self-energy.

The paper is organized as follows: In Secs. II A and II B, the Keldysh formalism and the correlation functions needed for the evaluation of the charge-state fractions are presented. In Sec. II C, the second-order self-energy is calculated. In Sec. II D, the particular case of bulk-plasmon-assisted processes is considered, where the bulk dielectric function appears automatically. In Sec. III, by using a simplified description of the solid response function, we show some results for a proton impacting on an Al jellium target, and the interplay between the resonant processes and the bulk-plasmon-assisted processes is analyzed. Finally, in Sec. V, some concluding remarks are presented.

II. THEORY

A. Keldysh formalism

In this section we introduce the formalism to calculate the neutralization rates for a one-state atom when it is scattered from a metal surface. The resonant, Auger, and plasmon-assisted channels, together with the effects of the dynamical evolution, are considered. We assume a classical trajectory for the ion which yields a time-dependent Hamiltonian; the Keldysh Green's-function formalism[9] is then the adequate method to calculate the population of the states for this non-equilibrium process. The total Hamiltonian can be written as

$$H = H_0 + H_1(t),$$

where H_0 is the noninteracting part involving the sum of the energy terms related with the ion and metal band states

$$H_0 = \varepsilon_a c_a^\dagger c_a + \sum_{\vec{k}} \varepsilon_{\vec{k}} c_{\vec{k}}^\dagger c_{\vec{k}}.$$

We have chosen the solid as the inertial reference system, then ε_a is the orbital energy plus the kinetic energy due to the ion velocity. The interaction Hamiltonian, $H_1(t)$ involves the resonant and the Augerlike terms, and the electron-electron Coulomb potential in the solid:

$$H_1(t) = \sum_{\vec{k}} [V_{\vec{k}a}(t) c_{\vec{k}}^\dagger c_a + \text{H.c.}] + \sum_{\vec{k},\vec{k}',\vec{k}''} [V_{\vec{k}\vec{k}'\vec{k}''a}(t) c_{\vec{k}}^\dagger c_{\vec{k}'}^\dagger c_{\vec{k}''} c_a + \text{H.c.}] + \tfrac{1}{2} \sum_{\vec{k},\vec{k}',\vec{k}'',\vec{k}'''} V_{\vec{k}\vec{k}'\vec{k}''\vec{k}'''} c_{\vec{k}}^\dagger c_{\vec{k}'}^\dagger c_{\vec{k}''} c_{\vec{k}'''}.$$

The resonant interaction is chosen to be a hopping potential:

$$V_{\vec{k}a}(t) = \langle \vec{k} | \frac{-Ze}{|r - R(t)|} | a(t) \rangle;$$

a more general one-electron potential term will not make a real difference in what follows. The Augerlike term is a two-electron potential between the solid and the ion states:

$$V_{\vec{k}\vec{k}'\vec{k}''a}(t) = \langle \vec{k} | \langle \vec{k}' | \frac{1}{|r - r'|} | \vec{k}'' \rangle | a(t) \rangle. \tag{1}$$

Finally, the two-electron potential between the band states has to be considered in order to include the plasmon-assisted neutralization channel, arising from the dynamic screening by the metal electrons:

$$V_{\vec{k}\vec{k}'\vec{k}''\vec{k}'''} = \langle \vec{k} | \langle \vec{k}' | \frac{1}{|r - r'|} | \vec{k}'' \rangle | \vec{k}''' \rangle. \tag{2}$$

It is worthwhile to point out that the atomic and band states involved in the evaluation of the transition amplitudes $V_{\vec{k}a}(t)$ and $V_{\vec{k}\vec{k}'\vec{k}''a}(t)$ should be orthogonalized states. To keep the usual commutative relations between the state creation and destruction operators, the electron field operator in real space must be expanded in a complete set $\{c_{\vec{k}}, c_a\}$, imposing the orthogonality condition.

The Keldysh formalism is a rigorous theory of nonequilibrium processes consisting of an extension of the usual diagrammatic techniques for calculating Green's functions. As clearly explained by Blandin, Nourtier, and Hone, the correlation functions defined for a time-dependent process do not fulfill Wick's theorem, and their diagrammatic expansion in terms of noninteracting functions is not valid. The Keldysh method solves this problem by introducing a correlation function evaluated in the variables s and s' that runs over the contour C shown in Fig. 1, that admits a diagrammatic expansion, and from which the usual two-time Green's functions can be extracted.[10] In the case we are interested in, the population of the atomic state as a function of time can be calculated through the evaluation of the following Keldysh Green's function:

$$G_a(s,s') = -i \langle 0 | T_c [\tilde{c}_a(s) \tilde{c}_a^\dagger(s') S_c] | 0 \rangle, \tag{3}$$

where T_c is the chronological ordering operator on the contour C

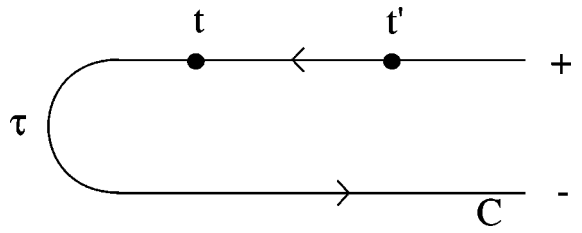

FIG. 1. Contour C defines the relation between the t and s variables. While s runs over the contour from $-\infty$ to ∞ , t runs from $-\infty$ to τ and again to $-\infty$. For each t variable, the upper and lower branches of the contour define a Keldysh Green's function.

$$T_c[\tilde{c}_a(s)\tilde{c}_a^{\dagger}(s')]=\begin{cases}\tilde{c}_a(s)\tilde{c}_a^{\dagger}(s') & \text{if } s>s' \\ -\tilde{c}_a^{\dagger}(s')\tilde{c}_a(s) & \text{if } s<s',\end{cases}$$

and S_c is the scattering operator defined as

$$S_c=T_c\ \exp\left[-i\int_c \tilde{H}_1(s)ds\right],$$

$\tilde{c}_a$ and $\tilde{H}_1$ being the atomic state destruction operator and the interaction potential in the interaction scheme, respectively.

The atomic and band states are mixed by the presence of $\tilde{H}_1$; then the Feynman perturbation expansion of Eq. (3) will give us a result in terms of the unperturbed Keldysh Green's functions

$$G_a^0(s,s')=-i\langle 0|T_c[\tilde{c}_a(s)\tilde{c}_a^{\dagger}(s')]|0\rangle$$

and

$$G_k^0(s,s')=-i\langle 0|T_c[\tilde{c}_k(s)\tilde{c}_k^{\dagger}(s')]|0\rangle.$$

A Dyson equation for $G_a(s,s')$, and consequently a self-energy $\Sigma(s,s')$, are defined:

$$G_a(s,s')=G_a^0(s,s')+\int_c G_a^0(s,s_1)\Sigma(s_1,s_2)\times G_a(s_2,s')ds_1ds_2. \tag{4}$$

The self-energy for the atom propagator has a straightforward perturbation expansion in powers of the interaction potential, and, as in the time-independent case, it is better to truncate the series expansion of the self-energy and to solve Eq. (4) rather than approximating the Green's function itself. Once $G_a(s,s')$ is calculated , it only remains to recover the real-time Green's functions from it. By using the fact that for each real time t, two values of s can be associated, the branches involved for s and s' give rise to four functions $G^{\alpha\beta}$, where α and β are $+$ or $-$ depending on the positions of s and s' on the upper $(+)$ and lower $(-)$ branches of the contour C. By applying T_c to the S_c definition, it is easy to arrive at the following expressions:

$$\begin{aligned}G_a^{++}&=G_a(t,t'),\\ G_a^{++}-G_a^{+-}&=G_a^r(t,t'),\\ G_a^{++}-G_a^{-+}&=G_a^a(t,t'),\\ G_a^{++}+G_a^{--}&=F(t,t'),\end{aligned} \tag{5}$$

where $G_a(t,t')=-i\langle\Psi(0)|T[c_a(t)c_a^{\dagger}(t')]|\Psi(0)\rangle$ is the causal two-time Green's function, where the fermionic operators are in the Heisenberg representation, and T is the usual chronological ordering operator. The other two Green's functions $G_a^r(t,t')$ and $G_a^a(t,t')$ are the retarded and advanced ones, respectively. $F(t,t')$ is related to the occupation of the atom-state. In order to evaluate the atom-state population as a function of time $n(t)$, it is better to deal with $F(t,t')$ instead of $G_a(t,t')$, which is not well defined at $t=t'$. The average occupation number can be calculated from $F(t,t')$ as follows:[10]

$$n(t)=\frac{[1-iF(t,t)]}{2}. \tag{6}$$

Similar relations are satisfied by the self-energy:

$$\begin{aligned}\Sigma^{++}+\Sigma^{+-}&=\Sigma^r(t,t'),\\ \Sigma^{++}+\Sigma^{-+}&=\Sigma^a(t,t'),\\ \Sigma^{++}+\Sigma^{--}&=\Omega(t,t').\end{aligned} \tag{7}$$

B. Equations of motion

The diagrammatic technique is a step-by-step method that gives us an approximated solution for $\Sigma(s,s')$, and through Eq. (7) approximations for $\Sigma^{a,r}(t,t')$ and $\Omega(t,t')$. It is more convenient to calculate $G_a^{a,r}$ and F directly instead of solving $G(s,s')$. This can be done through their equations of motion that are obtained by differentiating the time version of Eq. (4). For simplicity, we introduce the reduced Green's functions

$$g_a^{a,r}(t,t')=e^{i\int_{t'}^{t}\varepsilon_a(\tau)d\tau}G_a^{a,r}(t,t'),$$

$$f(t,t')=e^{i\int_{t'}^{t}\varepsilon_a(\tau)d\tau}F(t,t')$$

and similar expressions for the reduced self-energies $\epsilon^{a,r}$ and ω. The equations of motion for these new quantities are

$$i\frac{d}{dt}g_a^{a,r}(t,t')=\delta(t-t')+\int_{-\infty}^{\infty}\epsilon^{a,r}(t,t_1)g_a^{a,r}(t_1,t')dt_1,$$

$$i\frac{d}{dt}f(t,t')=\int_{-\infty}^{t'}\omega(t,t_1)g_a^a(t_1,t')dt_1+\int_{-\infty}^{t}\epsilon^r(t,t_1)f(t_1,t')dt_1,$$

with the following boundary conditions:

$$\begin{aligned}g_a^a(t,t')&=0 \quad \text{if } t'<t,\\ g_a^r(t,t')&=0 \quad \text{if } t'>t,\\ f(-\infty,t')&=[2n(-\infty)-1]g_a^a(-\infty,t').\end{aligned}$$

Several features are remarkable: (1) $g_a^{a,r}$ is solely determined by $\epsilon^{a,r}$, and is independent of the orbital initial popu-

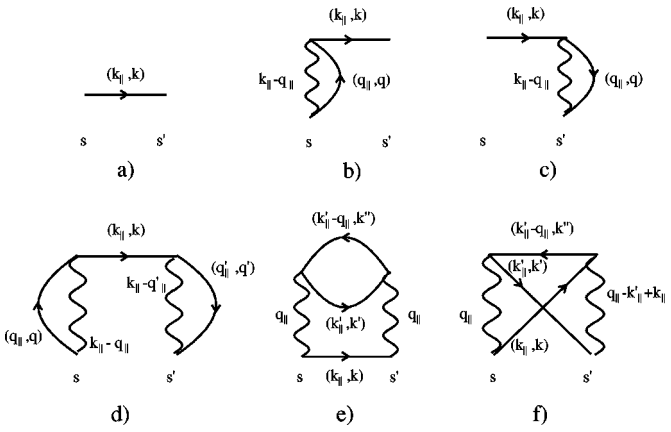

FIG. 2. Second-order self-energy diagrams. Solid lines are associated with band electron propagators, and waved lines with the Auger transition amplitudes. The points at the solid lines edges are resonant exchange amplitudes. Diagram (a) represents a pure resonant process. Diagrams (b) and (c) are interferences between resonant and Auger transitions. Diagrams (d)–(f) are associated with pure Auger processes. We refer to (e) as the direct Auger contribution, and (f) as the exchange Auger contribution to the self energy.

lation; therefore the orbital population cannot be extracted from these functions. (2) $f(t,t')$ is determined by $g_a^a(t_1,t')$ for $-\infty<t_1<t'$ with a boundary condition that depends on the initial population. (3) A similar equation of motion can be achieved for $f(t,t')$ as a function of $g_a^r(t_1,t')$ for $t'<t_1<\infty$, and a boundary condition that depends on the final population.

C. Self-energy

If we assume the solid to be a jellium, but consider explicitly the translational symmetry that remains in the direction parallel to the surface, the Auger potential term Eq. (1) can be written in its most general form as

$$\sum_{\vec{k},\vec{k}',q_\parallel\neq 0,k''} V^{q_\parallel}_{\vec{k},k',k'',a} c^\dagger_{\vec{k}} c^\dagger_{\vec{k}'} c_{(k'_\parallel-q_\parallel,k'')} c_a + \text{H.c.} \tag{8}$$

where now the solid index $\vec{k}=(k_\parallel,k)$ labels a state with components $k_\parallel$ and k parallel and normal, respectively. In this section, when the label k appears without the arrow, we refer to the normal component. Moreover, the Coulomb potential Eq. (2) becomes

$$\tfrac{1}{2}\sum_{\vec{k},\vec{k}',q_\parallel\neq 0,k'',k'''} V^{q_\parallel}_{k,k',k'',k'''} c^\dagger_{\vec{k}} c^\dagger_{\vec{k}'} c_{(k'_\parallel-q_\parallel,k'')} c_{(k_\parallel+q_\parallel,k''')}. \tag{9}$$

The atomic self-energy $\Sigma(s,s')$ up to a second order in the Auger and resonant potentials can be symbolized by the diagrams shown in Fig. 2, where solid lines are attached to noninteracting band propagators, and waved curves are attached to Auger interactions, while the points at the solid line edges represent resonant processes. Diagrams (a)–(d) have the peculiarity that only one electron is propagating in time; therefore they can be summed to give

$$\Sigma_R(s,s')=\sum_{\vec{k}} V'_{\vec{k},a}(t)^* V'_{\vec{k},a}(t') G^0_{\vec{k}}(s,s'), \tag{10}$$

where an effective resonant amplitude has been defined:

$$V'_{\vec{k},a}(t)=V_{\vec{k},a}(t)-\sum_{\vec{q}} V^{k_\parallel-q_\parallel}_{\vec{q},k,q,a}(t) n_{\vec{q}}. \tag{11}$$

Equation (10) comprises resonant processes, and those Auger transitions where the solid excitation does not propagate in time, along with the interference between them.

By using Eq. (7), it is straightforward to obtain the two-time self-energies

$$\Sigma^a_R(t,t')=i\Theta(t'-t)\sum_{\vec{k}} V'_{\vec{k}a}(t)^* V'_{\vec{k}a}(t') e^{-i\varepsilon_{\vec{k}}(t-t')},$$

$$\Sigma^r_R(t,t')=\Sigma^a_R(t',t)^*, \tag{12}$$

$$\Omega_R=-i\sum_{\vec{k}} V'_{\vec{k}a}(t)^* V'_{\vec{k}a}(t') e^{-i\varepsilon_{\vec{k}}(t-t')}(1-2n_{\vec{k}}).$$

The last two diagrams [Fig. 2(e) and 2(f)] represent Auger transitions assisted by an electron-hole excitation, where both electron and hole propagate in time. In Fig. 2(e), the transferred electron behaves like a free particle, and the solid polarization can be expressed, as in the LRA, through a response function. We will refer to this case as the direct Auger transition, and its contribution to the self-energy is

$$\Sigma_D(s,s')=-i\sum_{\vec{k},q_\parallel,k',k''} V^{q_\parallel}_{\vec{k},k',k'',a}(t)^* V^{q_\parallel}_{\vec{k},k',k'',a}(t') \times G^0_{\vec{k}}(s,s')\Pi^{q_\parallel}_{k',k''}(s,s'), \tag{13}$$

where we have introduced the polarization function

$$\Pi^{q_\parallel}_{k',k''}(s,s')=-i\sum_{k'_\parallel} G^0_{(k'_\parallel,k')}(s,s') G^0_{(k'_\parallel-q_\parallel,k'')}(s',s), \tag{14}$$

that is very similar to the one obtained in the LRA.

Finally, Fig. 2(f) symbolizes those processes where the recaptured electron is different from the one lost by the atom. These exchange processes give the following contribution to the total self-energy:

$$\Sigma_E(s,s')=-\sum_{\vec{k},\vec{k}',q_\parallel,q'_\parallel,k''} V^{q_\parallel}_{\vec{k},k',k'',a}(t)^* \times V^{q_\parallel-k'_\parallel+k_\parallel}_{\vec{k}',k,k'',a}(t') G^0_{\vec{k}}(s,s') G^0_{\vec{k}'}(s,s') \times G^0_{(k'_\parallel-q_\parallel,k'')}(s',s). \tag{15}$$

If the electron-electron Coulomb potential in the solid is disregarded, the second-order self-energy is the addition of Eq. (10) to Eqs. (13) and (15). Nevertheless, it is known from experimental observations that the plasmon-assisted transitions play an important role in the neutralization of ions. In addition, the linear response theory puts both electron-hole pair and plasmons in the same framework by

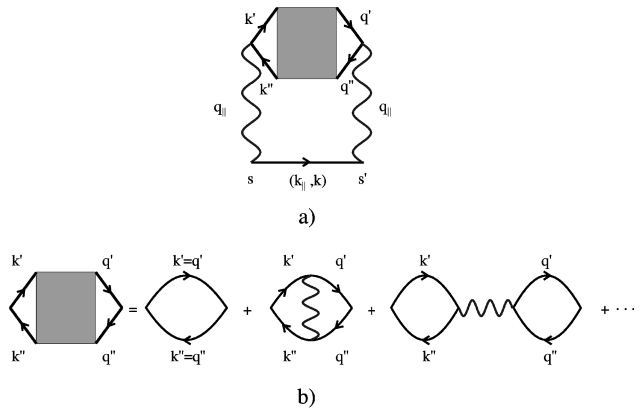

FIG. 3. (a) Diagrammatic representation of the direct Auger contribution to the self-energy when the Auger interaction lines are screened by the Coulomb potential between band states. The four vertex function represented by a filled square is the susceptibility function $\chi^{q_\parallel}_{k',k'',q',q''}$. (b) Diagrammatic expansion of $\chi^{q_\parallel}_{k',k'',q',q''}$ in terms of the Coulomb potential (waved lines).

defining the dielectric response function in a way that the solid behaves like an external body that provides the energy and momentum necessary to assure the transition. Following a similar procedure, we replace the Auger interactions with screened lines.[22] Figure 2(e) is then substituted by Fig. 3(a), where the four vertex function is expanded in terms of the Coulomb interaction in Fig. 3(b); the screening of Fig 2(f) gives four diagrams (Fig. 4). The effect of considering the electron exchange mechanism assisted by the collective and electron-hole pair excitation in the solid is just to replace the polarization function $\Pi^{q_\parallel}_{k',k''}(s,s')$ in Eq. (13) by the susceptibility function $\chi^{q_\parallel}_{k',k'',q',q''}(s,s')$, and the direct Auger self-energy becomes

$$\Sigma_D(s,s') = -i\sum_{\vec{k},q_\parallel}\sum_{k',k'',q',q''} V^{q_\parallel}_{\vec{k},k',k'',a}(t)^* \times V^{q_\parallel}_{\vec{k},q',q'',a}(t')G^0_{\vec{k}}(s,s')\chi^{q_\parallel}_{k',k'',q',q''}(s,s'). \tag{16}$$

As the unperturbed part of the Hamiltoninan and the interaction potential involved in the calculation of the susceptibility function are time independent, from the four two-time susceptibilities only one survives. In addition, it must be identical to that obtained in the LRA and a function of the time difference. Therefore, a Fourier transformation can be performed, and a frequency function $\chi^{q_\parallel}_{k',k'',q',q''}(\varpi)$ can be defined. The retarded piece of this function is closely related to the dielectric response function.[23] In Sec. II D, we present

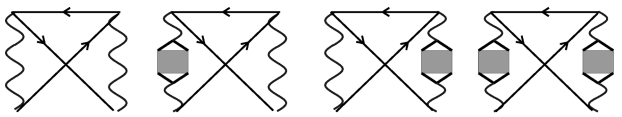

FIG. 4. When the Auger exchange diagram [Fig. 2(f)] is screened by the Coulomb potential, four terms appear. The first term is equal to the original one, the second and third terms are of the first order in the susceptibility function, and the fourth term is a second-order correction.

the form of the dielectric function when the solid wave functions are approximated by plane waves. Although the deduction is given for a particular case, the same procedure can be carried out when the breaking of symmetry due to the surface is considered.

The Auger exchange self-energy expressions are not presented here. They can be straightforwardly obtained as products of unperturbed Green's functions and susceptibility functions.

D. Bulk dynamical response

To keep the mathematics as simple as possible, but at the same time to give an example of the application of the formalism, we approximate the electron-hole pair wave functions by plane waves in the Auger and Coulomb potentials. As a direct consequence, no surface polarization will be obtained, that is to say, only bulk plasmons and electron hole excitations would be the product of the Auger exchange process. With this assumption, the Auger potential amplitude becomes

$$V_{\vec{k},\vec{q},a}(t) = \frac{4\pi}{q^2}\langle \vec{k}|e^{-i\vec{q}\vec{r}}|a(t)\rangle,$$

where $\vec{k}$ is now a three-dimensional vector, $\vec{q}$ is the momentum transferred during the process, and the Coulomb potential has the usual expression

$$\frac{1}{2}\sum_{\vec{k},\vec{k}',\vec{q}\neq 0}\frac{4\pi}{q^2}c^\dagger_{\vec{k}+\vec{q}}c^\dagger_{\vec{k}'-\vec{q}}c_{\vec{k}'}c_{\vec{k}}.$$

The effective resonant amplitude is reduced to

$$V'_{\vec{k}a}(t) = V_{\vec{k}a}(t) - \sum_{\vec{q}} V_{\vec{k}-\vec{q},\vec{q},a}(t)n_{\vec{k}-\vec{q}},$$

and the direct Auger self-energy becomes

$$\Sigma_D(s,s') = -i\sum_{\vec{k},\vec{q}} V_{\vec{k},\vec{q},a}(t)^* V_{\vec{k},\vec{q},a}(t')G^0_{\vec{k}}(s,s')\chi_{\vec{q}}(s,s'), \tag{17}$$

where the susceptibility depends on $\vec{q}$, the momentum transferred to the solid.

The four two-time self-energies become

$$\overline{\Sigma}_D(t,t') = -i\sum_{\vec{k},\vec{q}} V_{\vec{k},\vec{q},a}(t)^* V_{\vec{k},\vec{q},a}(t')\begin{pmatrix} G^{0++}_{\vec{k}}(t,t')\chi^{++}_{\vec{q}}(t,t') & -G^{0+-}_{\vec{k}}(t,t')\chi^{+-}_{\vec{q}}(t,t') \\ -G^{0-+}_{\vec{k}}(t,t')\chi^{-+}_{\vec{q}}(t,t') & G^{0--}_{\vec{k}}(t,t')\chi^{--}_{\vec{q}}(t,t')\end{pmatrix},$$

where the four $\chi_{\vec{q}}^{\alpha\beta}(t,t')$'s are not all independent. It can be shown that they have a self-energy character, therefore,

$$\chi_{\vec{q}}^{++}(t,t')=\Theta(t-t')\chi_{\vec{q}}^{-+}(t,t')+\Theta(t'-t)\chi_{\vec{q}}^{+-}(t,t'),$$

and, introducing the susceptibility Fourier transform $\chi^{++}(\vec{q},\varpi)$,

$$\chi^{++}(\vec{q},\varpi)=-\chi^{--}(\vec{q},\varpi)^*.$$

By using these two relations, the self-energy advanced piece can be written in terms of $\chi^{++}(\vec{q},\varpi)$ as

$$\Sigma_D^a(t,t')=-\Theta(t'-t)\sum_{\vec{k},\vec{q}} V_{\vec{k},\vec{q},a}(t)^*V_{\vec{k},\vec{q},a}(t')\times\int_{-\infty}^{\infty}\frac{d\varpi}{2\pi}e^{-i(\varepsilon_{\vec{k}}+\varpi)(t-t')}[n_{\vec{k}}\,\chi^{++}(\vec{q},\varpi)-(1-n_{\vec{k}})\chi^{++}(\vec{q},\varpi)^*], \tag{18}$$

and similar expressions can be obtained for Σ_D^r and Ω_D.

It is remarkable that the two-time self-energies depend exclusively on χ^{++}, which is the jellium susceptibility in the time-independent case. This is a direct consequence of the time-independent character of the Coulomb potential, and of the way the Auger amplitudes were screened. For positive frequency values $\chi^{++}(\vec{q},\varpi)=\chi^r(\vec{q},\varpi)$, where χ^r is the retarded piece given by $\chi^r=1/\varepsilon(\vec{q},\varpi)-1$, with $\varepsilon(\vec{q},\varpi)$ the dielectric response function. Using

$$\chi^{++}(\vec{q},\varpi)=\frac{2}{2\pi}\int_0^{\infty}d\varpi'\,\mathrm{Im}[\chi^{++}(\vec{q},\varpi')]\times\left(\frac{1}{\varpi'-\varpi-i\eta}+\frac{1}{\varpi'+\varpi-i\eta}\right),$$

the ϖ integration can be reduced to only positive values, and $\chi^{++}(\vec{q},\varpi)$ can be replaced by χ^r.[23] Finally, the direct Auger self-energies become

$$\Sigma_D^a(t,t')=i\Theta(t'-t)\sum_{\vec{k},\vec{q}} V_{\vec{k},\vec{q},a}(t)^*V_{\vec{k},\vec{q},a}(t')\times\int_0^{\infty}\frac{d\varpi}{2\pi}e^{-i\varepsilon_{\vec{k}}(t-t')}2\,\mathrm{Im}\left(\frac{-1}{\varepsilon(\vec{q},\varpi)}\right)[n_{\vec{k}}e^{i\varpi(t-t')}+(1-n_{\vec{k}})e^{-i\varpi(t-t')}],$$

$$\Sigma_D^r(t,t')=\Sigma_D^a(t,t')^*, \tag{19}$$

$$\Omega(t,t')=-i\sum_{\vec{k},\vec{q}} V_{\vec{k},\vec{q},a}(t)^*V_{\vec{k},\vec{q},a}(t')\times\int_0^{\infty}\frac{d\varpi}{2\pi}e^{-i\varepsilon_{\vec{k}}(t-t')}2\,\mathrm{Im}\left(\frac{-1}{\varepsilon(\vec{q},\varpi)}\right)\times[n_{\vec{k}}\,e^{i\varpi(t-t')}-(1-n_{\vec{k}})e^{-i\varpi(t-t')}].$$

These are our final expressions. They give the direct Auger self-energies as a product of three meaningful terms: (1) $V^*_{\vec{k},\vec{q},a}V_{\vec{k},\vec{q},a}$, the electronic exchange probability assisted by an excitation of momentum $\vec{q}$, (2) $\mathrm{Im}[-1/\varepsilon(\vec{q},\varpi)]$, the excitation probability that takes into account the response of the solid as an interacting electronic system; and (3) $(1-n_{\vec{k}})$ and $n_{\vec{k}}$, the condition imposed by the Pauli principle that an electron must be captured from an occupied state and lost to an empty one. The direct Auger contribution to the self-energy can be viewed as the product of the interaction of three bodies: the ion with a fixed classical trajectory, the transferred electron, and finally the solid that acts like an energy and momentum bath. These components of the system interact when a transfer process occurs, meanwhile, they propagate following their own dynamics: the transferred electron behaves like a free particle, while the excitation induced in the medium has a time dependence fixed by its energy and momentum. These phases are considered in the Keldysh approach, so the quantum character of the transfer process is preserved. Conversely, within the rate-equation approximation the solid response is instantaneous and static; the excitation induced in the medium does not propagate in time and the quantum character of the process is lost.

In the exchange Auger processes [Figs. 2(f) and 4] the system cannot be separated into different components because of the undistinguishable character of the electrons, the time evolution of the particles between successive interactions appears to be crucial, and the contribution to the self-energy to be of the same order as the direct Auger contribution. With the Keldysh formalism one can handle these two contributions to the self-energy on an equal footing along with the interference between them.

Other important improvements with respect to the rate-equation model can be stressed. Equation (19) can be written as the sum of two contribution: the positive frequency term (left side), can be associated with the capture process, and the negative frequency term (right side), which can be associated with loss processes. When the calculation of the atomic population is performed, these contributions mix and interfere with each other to give the final result. Conversely, in the rate-equation approach the contributions of capture and loss processes are artificially separated because their influence on the evolution of the atomic population is expressed through probabilities. Moreover, in a rate-equation approach the probabilities govern the time evolution of the atomic population, while in the Keldysh formalism the full quantum character of the scattering is preserved through the time dependence of the probability amplitudes.

It is worthwhile to point out that in the stationary case of an atom moving in an infinite jellium the Auger amplitudes' time dependence is a phase factor. It is straightforward to show that in that case Eq. (19) reduces to those expressions

proposed by Echenique, Flores, and Ritchie calculated from a different point of view.[24]

The total self-energy is

$$\Sigma_T(t,t')=\Sigma_R(t,t')+\Sigma_D(t,t')+\Sigma_E(t,t'), \qquad (20)$$

where $\Sigma_R(t,t')$ is defined in Eq. (12), $\Sigma_D(t,t')$ in Eqs. (19) or (16) when the surface effects are taken into account, and $\Sigma_E(t,t')$ in Eq. (15).

Equation (20) is the central result of this work, where the most relevant charge-exchange mechanisms have been incorporated into the same framework, giving place to interferences between them in a natural way within the formalism. The dynamical character of the scattering process is taken into account together with the dynamical response of the solid, allowing not only for an Auger neutralization process but also for a plasmon-assisted neutralization one.

In the Keldysh approach, the self-energy contains all the physical effects involved in the description of the system. Its great advantage resides in its additive character: new mechanisms can be incorporated simply by adding new terms. The way to improve the formalism becomes clear: better self-energies will give better results. In our case, for example, a more realistic description can be obtained by replacing the unperturbed propagators of the transferred electron in Figs. 3(a) and 4, with propagators screened by the electron-electron potential. Then the transferred electron will propagate between successive exchange processes as an interacting particle and not as a free one. Moreover, the perturbation series in the interaction potential H_I can be continued to higher orders, going beyond the LRA approximation, and realistic image effects can then be incorporated. We believe that the self-energy proposed in Eq. (20) is complex enough to describe the problem, and the surface susceptibility function allows us to handle bulk- and surface-plasmon-assisted transitions along with the resonant and Auger mechanism. Finally, by slightly changing the interaction potential and following similar steps, Auger transitions with electron-hole creation in the atom or quasiresonant mechanisms can also be incorporated.

III. RESULTS

The aim of this section is to present an application of the formalism to a simple model of an ion-solid collision. Accuracy in the description of the actual process is sacrificed on behalf of simplicity. At low ion velocities it is expected that the resonant channel is more important than the Auger mechanism, while at high velocities the situation is inverted. As an example of the interplay of the different channels involved in the ion neutralization, we perform the calculation at an intermediate ion velocity, at which both channels are expected to be equally important. We consider the case of a one-state ion that impacts on an Al target, considering only bulk dynamical response. This restriction allows us to carry out a simple preliminary calculation in order to clarify the role played by the bulk-assisted transitions. The comparison with the experimental results requires a more rigorous description of the surface response function, which is left for a forthcoming paper.

The resonant and Auger self-energies are calculated from Eqs. (12) and (19), approximating the solid wave functions by plane waves, and the atomic orbital by a $1s$ wave function. The effect of the surface is included by multiplying the transition amplitudes by exponentials decreasing with the ion-surface distance.[25] With this assumption, $V'_{\vec{k}a}(t)$ becomes equal to

$$V'_{\vec{k}a}(t)=e^{-g_R(z(t))}\frac{Z_e^{5/2}\sqrt{2}}{\pi}\,\frac{e^{-i(\vec{k}-\vec{v})\vec{v}t}}{Z_e^2+|\vec{k}-\vec{v}|^2}\times\left[1-\frac{2}{\pi}\,\frac{k_F+(k^2-k_F^2)/2k\,\ln\left|\frac{k_f-k}{k_f+k}\right|}{Z_e^2+|\vec{k}-\vec{v}|^2}\right],$$

where Z_e is the ion charge, $\vec{v}$ is the ion velocity, k_F is the Fermi momentum, and $g_R(z(t))$ is a function of the ion trajectory. The second term in the expression in brackets is the correction to the resonant amplitude due to the Auger transition [Eq. (11)]. The Auger potential amplitude can be written as

$$V_{\vec{k},\vec{q},a}=e^{-g_A(z(t))}\frac{(2Z_e)^{5/2}}{(2\pi)^4}e^{-i(\vec{k}-\vec{v}+\vec{q})\vec{v}t}\;\;h(\vec{k},\vec{q}),$$

where

$$h(\vec{k},\vec{q})=\frac{4\pi}{q^2[Z_e^2+|\vec{k}-\vec{v}+\vec{q}|^2]^2}$$

is approximated by a function that depends only on the $\vec{k}$ and $\vec{q}$ modulus in order to simplify the numerical calculations. The error introduced by this approximation is expected to be small, because the time-dependent phase factor remains untouched; in addition, in the infinite jellium case this phase yields the energy conservation rule that governs the qualitative behavior of the transition rates. Finally, we take the dielectric response function in the plasmon-pole approximation.[24] As a direct consequence, a cutoff is introduced in the excitation energies equal to the plasmon frequency. In Sec. II, we pointed out that the atomic and solid states involved in the evaluation of the resonant and Auger amplitudes should be orthogonal; however, in this preliminary calculation, and to keep the burden of the numerical calculations to a minimum, we use nonorthogonalized wave functions. The order of magnitude of the coupling terms will not be modified when band states are orthogonalized to the atomic orbital, although for small momentum transfers a reduction of the coupling strength is expected.

Hereinafter, we suppose that the ion has a charge $Z_e=1$, and impacts on the surface with a glancing angle φ and a constant normal velocity up to a turning point z_0, from where it is specularly reflected. Then, $g_R(z(t))$ and $g_A(z(t))$ are both equal to

$$g_{R,A}(z(t))=\gamma(z_0+v_z|t|),$$

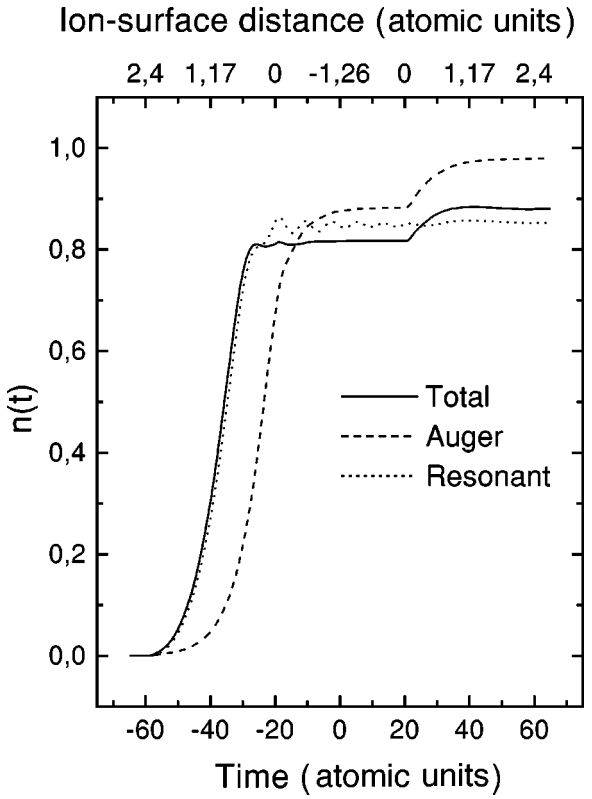

FIG. 5. The atomic occupation number is shown as a function of time for an ion velocity of 0.5 a.u., an incidence angle $\varphi = 7°$ and an energy level $\varepsilon_a = 0.25$ a.u. The solid line is the result when the full interaction is considered, while the dashed (dotted) line is the result when Auger (resonant) interaction is considered alone. The ion-surface distance is also shown.

with $\gamma = 1.3$ a.u. for Al.[25] Following Kimura,[26] we assume an incidence-angle-dependent turning point at z_0. By increasing φ, the penetration into the solid increases and z_0 becomes more negative.

Figure 5 gives the orbital population as a function of time $n(t)$ for an ion velocity of 0.5 a.u., an incidence angle of $\varphi = 7°$, and an energy level located at the middle of the valence band, $\varepsilon_a = 0.25$ a.u. with respect to the Al band bottom. The solid line is the result obtained when the full interaction is considered, the dashed line the result when only Auger processes are active, and the dotted line the result when only resonant processes are taken into account. Values of the ion-surface distance are shown for different times. The trajectory of specular reflection has the turning point placed at $z_0 = -1.26$ a.u. inside the jellium. It must be noticed that the turning point is above the first layer of atoms, located more than 2 a.u. inside the jellium edge. The resonant channel opens first, while the Auger interaction becomes important only for distances closer to the surface. This is evidence of the longer range of the resonant interaction as compared with the Auger interaction for these collision parameters. As we will see in Fig. 7, the interplay between both channels strongly depends on the position of the orbital energy with respect to the solid band. At the beginning of the trajectory, the full interaction occupation number is slightly larger than the resonant one. The Auger interaction acts as a capture channel because $n(t)$ is smaller than its bulk equilibrium value. When the ion penetrates the jellium, both Auger and solid lines reach a plateau and a dynamic charge equilibrium is achieved, the orbital occupation number is independent of the initial conditions, and its value corresponds to the infinite jellium case. The resonant neutralization tends to an equilibrium value in an oscillatory way inside the jellium, but does not achieve a constant value while the ion stays inside. Finally, as the interaction is turned off, the orbital populations adjust to their final values by increasing the occupation numbers. It is remarkable that the bulk equilibrium value for the full interaction is lower than the Auger and resonant bulk values. From a rate-equation calculation it could be expected that the full interaction line falls always between the Auger and resonant results in an equilibrium situation because then the depopulation of the state due to one of the exchange channels would be compensated for by the other. Therefore, the effect we find in our calculations should be a direct consequence of the interference between the Auger and resonant processes, which is well taken into account by the Keldysh formalism.

For the parameters chosen for the collision, the ion ends up almost completely neutralized; both channels are equally important, and the total final population lies between the Auger and resonant final values as the rate-equation approach predicts. The resonant interaction appears to be stronger, although the occupation number in the equilibrium situation is similar for both channels when they are treated solely. This is not a contradiction; the equilibrium value is related not to the intensity of the interaction but to the relative strength between the capture and loss parts of the mechanism.

The oscillations of the atomic population as a function of time in the resonant result are typical of one-electron exchange processes, as are well known in ion-atom collisions. In the simplest model of the electron exchange between two levels with energy separation ΔE and mean coupling $\overline{V}$, it is easy to see that the capture probability has the following time dependence;[27]

$$P_c(t) \sim \left(\frac{\overline{V}}{\Gamma}\right) \sin(\Gamma t)^2, \tag{21}$$

with a frequency Γ given by $\Gamma^2 = (\Delta E/2)^2 + \overline{V}^{\,2}$. When the interaction with a band is considered, an estimation of the capture probability time dependence can be obtain by integrating contributions like Eq. (21) over the band energies. Therefore, the oscillations will be important in the narrow-band case while they will be washed out for a wide band. These considerations apply to the one-electron resonant channel. Conversely, the Auger channel opens up two-electron transitions, so the energy separation between initial and final states is not limited by the bandwidth, which explains the absence of oscillations in the atomic occupation number of Figs. 5 and 6.

The final occupation number $n(\infty)$ as a function of φ is shown in Fig. 6 where $\varepsilon_a = 0.25$ a.u. and $v = 0.5$ a.u. Dotted and solid lines correspond to initially unoccupied and occupied states, respectively. As a general behavior, for grazing incidence, $n(\infty)$ reaches a value that is independent of the initial condition; the effective interacting time is large enough to assure a dynamic equilibrium. When the incidence angle increases, the effective time decreases, and the final

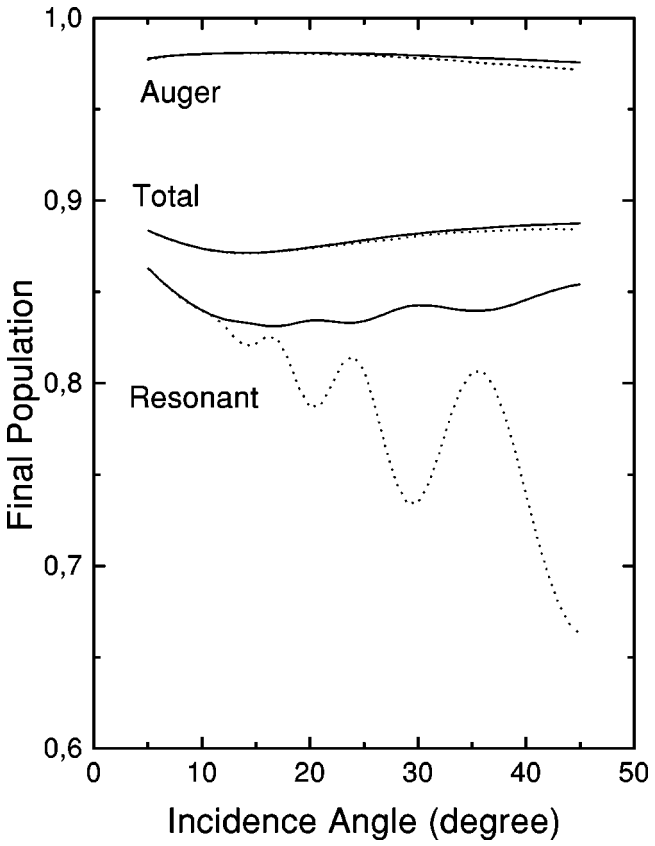

FIG. 6. The final occupation number $n(\infty)$ as a function of the incidence angle φ is shown for an ion velocity of 0.5 a.u. and an orbital energy $\varepsilon_a = 0.25$ a.u. The solid (dotted) line corresponds to an initial orbital population $n(t_0)=1[n(t_0)=0]$.

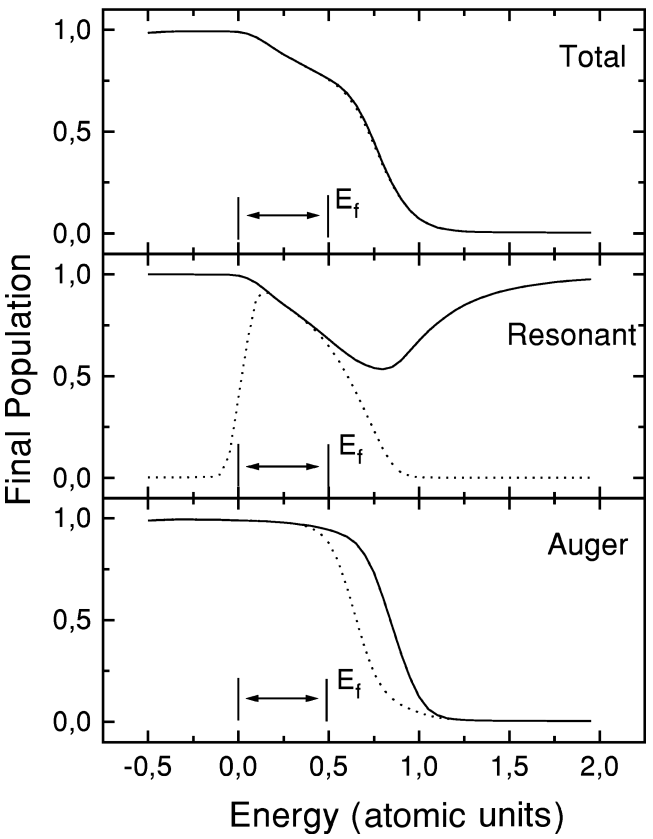

FIG. 7. The final occupation number $n(\infty)$ as a function of the orbital energy for an ion velocity of 0.5 a.u. and an incidence angle $\varphi = 7°$. Solid (dotted) line corresponds to an initial orbital population $n(t_0)=1[n(t_0)=0]$.

populations show a dependence on the initial occupation of the atomic state. Then the dynamical effects on the evolution of the atomic population are expected to be important, and the use of the Keldysh formalism to be necessary. When only the one-electron resonant channel is considered, the atomic population shows a marked oscillatory dependence on φ. The oscillations of the results when the atomic state is initially empty or occupied are in counterphase. The electronic charge fluctuates in time between the orbital and the band with a characteristic frequency, Eq. (21), so if the orbital is initially occupied, at a half-period the state will be emptied, resembling an unoccupied initial condition. When the Auger process is incorporated into the description, the phase coherence in the buildup of the atomic amplitude is destroyed, and the oscillations disappear, as is shown in Fig. 5.

Figure 7 analyzes the ε_a dependence of the final population for an ion impacting with $\varphi = 7°$ and $v = 0.5$ a.u. Again, dotted and solid lines correspond to initially unoccupied and occupied states, respectively. When only the resonant channel is turned on, the final population differs from its original value only when the orbital energy is close to or into the band. Otherwise, the resonant coupling is so weak that, due to the finite interacting time, its effect becomes negligible. A dynamic equilibrium condition is achieved when the orbital energy is close to the middle of the band, where both capture and loss processes make a significant contribution. On the other hand, the Auger channel is important through the entire energy range. When ε_a is below the bottom of the band, the loss processes are forbidden, and the ion finishes neutralized in any case. Only when the orbital energy exceeds a cutoff determined by k_F, v, and the plasma frequency ω_P, do the loss processes contributions cease to be negligible. At larger energies, the orbital ends up depopulated even when it was initially occupied. When the orbital energy is close to and slightly above the Fermi level, the final occupation number is sensitive to the initial conditions. The interaction time is not long enough, and a dynamic equilibrium inside the jellium is not achieved. It is in this case that the use of the Keldysh formalism becomes crucial for obtaining correct answers. Finally, the full interaction calculations follow the Auger results in almost the entire energy range except when the orbital energy lies in the band. Here the joined effect of both interactions make the final population independent of the initial condition.

Summarizing, at the ion velocity considered, the Auger channel governs the ion population when the orbital energy falls outside the jellium band. Nevertheless, both channels become important, and the interference between them must be considered when the orbital energy is close to or into the band. Therefore, the weight of each channel is not only determined by the ion velocity but by the position of the atomic level with respect to the solid band. The calculations of the final population as a function of φ indicate that the dynamical evolution of $n(t)$ may be important at large incidence angles, where an equilibrium situation is not achieved. It should also be stressed that the sudden turn on and off of the interactions as the ion is scattered by the surface is an irre-

versible process; therefore, the use of the Keldysh formalism is highly recommended in all cases.

IV. CONCLUSIONS

The Keldysh formalism goes beyond the rate-equation calculations by considering the dynamical effects introduced by the scattering process itself, and provides a direct way to approximate and improve the calculation of the correlation functions . We have presented a method based on this formalism that contains the Auger, resonant, and plasmon-assisted channels for the neutralization of atoms colliding with metal surfaces. The approach is based on the calculation of the atomic Keldysh self-energies by using its Feynmann diagrammatic expansion in terms of the interaction potential. A second-order self-energy was calculated as the sum of resonant, Auger, and interference contributions, and an effective resonant amplitude was obtained that incorporates those Auger processes with a resonantlike behavior. The plasmon-assisted channel was introduced by screening the Auger interaction lines of the Feynman diagrams with the Coulomb potential between band states, and its effect on the self-energies appears through a surface susceptibility function. Therefore, both Auger and plasmon-assisted processes appears, as in the LRA, as nonseparable excitations of the solid band.

The analysis shown in Sec. II C is quite general, and considers the breakdown in the translational symmetry in the normal direction for the coupling amplitudes and the collective excitations. In this case, we found that the surface polarization function $\Pi^{q_\parallel}_{k',k''}$ depends on two normal indexes k' and k'', while the surface susceptibility function $\chi^{q_\parallel}_{k',k'',q',q''}$ depends on four indexes. On the other hand, when only bulk excitations are considered (Sec. II D) both polarization and susceptibility functions depend on the excitation wave vector $\vec{q}$. It is clear that the surface susceptibility function contains surfacelike excitations, surface plasmons, and bulklike excitations, electron-hole pair creation or bulk plasmons, and is the function to be used when a collision with a surface is studied. Unfortunately, the great number of integrals involved discourages the use of this function, and approximations by bulk response functions are very common.

Finally, we analyzed the interplay of the resonant and Auger processes for a H^+/Al collision at intermediate ion velocities as a function of the orbital energy and the incidence angle. We found that both channels appear to be important, and the interference between them non-negligible.

ACKNOWLEDGMENTS

We thank Dr. Gonzalo Gómez for fruitful discussions. One of the authors (E.C.G.) wishes to acknowledge financial support from CONICET and UNL through Grant Nos. 4800-1000 and 94-E12, respectively.

[1] R. L. Erickson and D. P. Smith, Phys. Rev. Lett. **34**, 297 (1975).
[2] R. Souda, M. Aono, C. Oshima, S. Otani, and Y. Ishizawa, Surf. Sci. **150**, 159 (1985); **176**, 657 (1986); **179**, 199 (1987).
[3] L. Los and J. J. C. Geerlings, Phys. Rep. **190**, 3 (1990).
[4] S. N. Mikhailov, L. C. A. van der Oetelaar, and H. H. Brongersma, Nucl. Instrum. Methods Phys. Res. B **85**, 420 (1994).
[5] R. A. Baragiola and C. A. Dukes, Phys. Rev. Lett. **76**, 2547 (1996).
[6] P. M. Echenique, R. H. Ritchie, and W. Brandt, Phys. Rev. B **20**, 2567 (1979); A. Mazarro, P. M. Echenique, and R. M. Ritchie, *ibid.* **27**, 4117 (1983); F. J. García de Abajo and P. M. Echenique, *ibid.* **46**, 2663 (1992).
[7] P. M. Echenique, R. M. Nieminene, and R. H. Ritchie, Solid State Commun. **37**, 779 (1981); P. M. Echenique and M. E. Uranga, in *Density Functional Theory of Stopping Power*, Vol. 271 of *NATO Advanced Study Institue Seres B: Physics*, edited by A. Gras-Marti, H. M. Urbassek, Néstor R. Arista, and F. Flores (Plenum, New York, 1991).
[8] E. G. Overbosch, B. Rasser, A. D. Tenner and J. Los, Surf. Sci. **92**, 310 (1980); R. Brako and D. M. Newns, *ibid.* **108**, 253 (1981); J. J. C. Greelings, J. Los, J. P. Gauyacq, and N. M. Temme, *ibid.* **172**, 257 (1986).
[9] L. V. Keldysh, Zh. Éksp. Teor. Fiz. **47**, 1515 (1964) [Sov. Phys. JETP **20**, 1018 (1965)].
[10] A. Blandin, A. Nourtier, and D. W. Hone, J. Phys. (Paris) **37**, 369 (1976).
[11] E. A. García, E. C. Goldberg, and M. C. G. Passeggi, Surf. Sci. **325**, 311 (1995); E. A. García, P. G. Bolcatto, and E. C. Goldberg, Phys. Rev. B **52**, 16 924 (1995).
[12] H. Shao, D. C. Langreth, and P. Norlander, Phys. Rev. B **49**, 13 948 (1994).
[13] J. Merino, N. Lorente, F. Flores, and M. Yu Gusev, Nucl. Instrum. Methods Phys. Res. B **125**, 288 (1997); N. Lorente, J. Merino, F. Flores, and M. Yu. Gusev;, *ibid.* **125**, 277 (1997).
[14] E. C. Goldberg and F. Flores, Phys. Rev. B **45**, 8657 (1992); E. C. Goldberg and M. C. Passeggi, J. Phys.: Condens. Matter **8**, 7637 (1996).
[15] K. J. Snowdon, R. Hentschke, A. Narmann, and W. Heiland, Surf. Sci. **173**, 581 (1986).
[16] A. A. Almulhem and M. D. Girardeau, Surf. Sci. **210**, 138 (1989); F. A. Gutierrez, *ibid.* **370**, 77 (1997).
[17] R. Zimmy, Z. L. Miskovic, N. N. Nedeljkovic, and Lj. D. Nedeljkovic, Surf. Sci. **255**, 135 (1991).
[18] R. Monreal and N. Lorente, Phys. Rev. B **52**, 4760 (1995); N. Lorente and R. Monreal, Surf. Sci. **370**, 324 (1997); N. Lorente and R. Monreal, Phys. Rev. B **53**, 9622 (1996).
[19] K. Makoshi and H. Kaji, Prog. Theor. Phys. Suppl. **106**, 327 (1991).
[20] G. D. Mahan, Comments Condens. Matter Phys. **16**, 333 (1994).
[21] D. Pines and P. Nozières, *The Theory of Quantum Liquids* (Benjamin, Reading MA, 1966).
[22] Gerarld D. Mahan, *Many-Particle Physics* (Plenum, New York 1990).
[23] A. L. Fetter and J. D. Walecka, *Quantum Theory of Many Particle Systems* (McGraw-Hill, New York, 1971).
[24] P. M. Echenique, F. Flores, and R. H. Ritchie, Solid State Phys. **43**, 229 (1990).
[25] M. Alducin, A. Arnau, and P. M. Echenique, Nucl. Instrum.

Methods Phys. Res. B **67**, 157 (1992).
[26] K. Kimura, M. Haseqawa, and M. Mannami, Phys. Rev. B **36**, 7 (1987).
[27] M. R. C. McDowell and J. P. Coleman, *Introduction to the Theory of Ion Atom Collisions* (North Holland, Amsterdam, 1970); B. H. Bransden and M. R. C. McDowell, *Charge Exchange and the Theory of Ion-Atom Collisions* (Oxford University Press, Oxford, 1992).